Enhanced percutaneous absorption of cilostazol nanocrystals using aqueous gel patch systems and clarification of the absorption mechanism

CHIAKI YOSHIOKA, YOSHIMASA ITO and NORIAKI NAGAI

Faculty of Pharmacy, Kindai University, Higashi-Osaka, Osaka 577-8502, Japan

Received October 19, 2017; Accepted January 12, 2018

DOI: 10.3892/etm.2018.5820

Abstract. Cilostazol (CLZ), an anti-platelet agent, is primarily used following the onset of cerebral infarction. However, as CLZ is only marginally soluble in water, a strategy for patients with serious secondary conditions, such as impaired consciousness or aphagia, is required. In the present study, topical formulations containing CLZ nanocrystals (CLZ_{nano}) were designed to enhance percutaneous absorption. In addition, the mechanism of penetration of CLZ_{nano} through rat skin was investigated. A topical formulation containing CLZ nanoparticles (CLZ_{nano} gel patch) was prepared using a combination of recrystallization and ball milling of an aqueous gel. The particle size of CLZ_{nano} was 74.5±6.2 nm (mean ± standard deviation). The concentration of permeated CLZ_{nano} and penetration mechanism of the nanocrystals were measured in a percutaneous absorption experiment. The amount of penetrated CLZ, the penetration rate (J_c), the penetration coefficient through the skin (K_p) and the skin/preparation partition coefficient (K_m) for the CLZ_{nano} gel patch were all significantly higher than those of the CLZ powder (CLZ_{micro}) gel patch, the CLZ_{nano} ointment and the CLZ_{micro} ointment. In *in vitro* percutaneous penetration experiments on the CLZ_{nano} gel patches, there was a positive correlation between the number of CLZ_{nano}. Following the application of the CLZ_{nano} gel patch on rat skin, 98% of penetrated CLZ was observed in nanoparticle form; for the CLZ_{micro} gel patch, this figure was 9%. In addition, the CLZ concentrations in the plasma of rats administered the CLZ_{nano} gel patches were significantly higher than those of rats administered the CLZ_{nano} CP gel and PEG ointments. It was suggested that CLZ_{nano} (diameter <100 nm) were transferred through the intracellular spaces in the skin and then into peripheral blood vessels. To the best of our knowledge, this is the first report to elucidate the mechanism of the percutaneous penetration of nanocrystal medicines.

Correspondence to: Dr Noriaki Nagai, Faculty of Pharmacy, Kindai University, 3-4-1 Kowakae, Higashi-Osaka, Osaka 577-8502, Japan
E-mail: nagai_n@phar.kindai.ac.jp

Abbreviations: CP, carbopol; CLZ, cilostazol; CLZ_{micro}, CLZ powder; CLZ_{nano}, CLZ nanocrystals; HPβCD, 2-hydoxypropyl-β-cyclodextrin; k_a, absorption rate constant; K_p, penetration coefficient through the skin; MC, methylcellulose; PEG, polyethylene glycol; SPM, scanning probe microscope

Key words: cilostazol, nanocrystal, aqueous gel patch, absorption mechanism

Introduction

Cilostazol (6-[4-(1-cyclohexyl-1H-tetrazol-5-yl)butoxy]-3,4-dihydrocarbostyril, CLZ) is known to exert anti-platelet aggregation and vasodilatory effects with minimal cardiac effects (1). Therefore, CLZ has been used as a therapeutic agent for the improvement of symptoms in conditions such as cancer (2), pain accompanying chronic arterial obstruction (3), and for the amelioration (4) and, prevention of cerebral infarction (5). The agent is only administered orally because of its low water- solubility (6). However, most patients with cerebral infarction have serious secondary conditions, such as impaired consciousness or aphagia (7). Thus, sufficient blood concentration and effects cannot be obtained with commercially available CLZ tablets.

Cataplasms can be classified into two classes a transdermal absorption type and a locally acting type (8). In particular, the transdermal drug delivery patch systems have been used for various clinical treatments, such as asthma, angina, and smoking cessation (9). Transdermal absorption preparations offer several advantages: They are not subjected to the first-pass effect, but are simply applied and switched on or off in the body; ensure sustained release; and improve patient quality of life through sustained effects (8). The skin consists of the cuticle, the corium the tela subcutanea and nerves, blood vessels, and lymph vessels (10). The transdermal drug delivery patch system acts by penetrating the stratum corneum, after which the medicine is absorbed into the blood.

Many methods have been used to enhance the bioavailability of sparingly water-soluble medicaments, in particular, and nanoscale systems such as liposomes, micelles, nanocrystals, and dendrimers have been proposed as drug carriers for transdermal drug delivery systems (11).

Recently, a transdermal delivery system using nanoparticles was reported. The available pathways for the penetration of the drug through the stratum corneum are the transcellular, intracellular, and transaccessory pathways (12,13). The transcellular pathway appears to be the main pathway (12,13). The

spaces between the cells are reported to be 50-70 nm (14). Therefore, the solid drug particles that are approximately the same size as the spaces between the cells, pass through the space and into peripheral blood vessels (15). Thus, nanocrystals improve bioavailability. After consideration of these reports, we aimed to prepare aqueous gel patches containing CLZ nanocrystals (CLZ_{nano}) with a particle size of <100 nm.

In this study, we designed topical formulations containing CLZ_{nano} and investigated the penetration and the retention of CLZ in rat blood after the administration of CLZ_{nano} gel patches in comparison with gelling agents for general-purpose bases. Moreover, we clarified the mechanism of the transport system of CLZ_{nano} through rat skin.

Materials and methods

Materials. CLZ powder (CLZ_{micro}) was kindly provided by Otsuka Pharmaceutical Co., Ltd. (Tokyo, Japan). 2-Hydoxypropyl-β-cyclodextrin (HPβCD) was purchased from Nihon Shokuhin Kako Co., Ltd. (Tokyo, Japan), low-substituted methylcellulose (MC) was provided by Shin-Etsu Chemical Co., Ltd. (Tokyo, Japan), and docusate sodium (DS) was obtained from Sigma Co., Inc. (Tokyo, Japan). All other chemicals used were of the highest purity commercially available.

Animals. Seven-week-old male Wistar rats were used in this study (SLC Inc., Shizuoka, Japan). The animals were housed under standard conditions (12 h/day of fluorescent light (7:00 a.m.-7:00 p.m.) and 25±1˚C) and allowed free access to a commercial diet (CR-3; Clea Japan Inc., Tokyo, Japan) and water. All procedures were approved by and performed in accordance with the Kindai University School of Pharmacy Committee for the Care and Use of Laboratory Animals (approval no. KAPS-25-002).

Preparation of the CLZ_{nano} formulation. Recrystallized CLZ was prepared as follows (16): CLZ (0.5 g) was dissolved in 50% ethanol (50 ml) at 120˚C, and the extracted CLZ was placed in a sonicator (Yamato Science Co., Ltd, Tokyo, Japan) for 5 sec and allowed to stand for 24 h. Thereafter, CLZ was collected by filtration (recovery rate: 92.3%). Nanocrystals of CLZ (CLZ_{nano}) were prepared by using zirconia balls and a Pulverisette 7 Planetary Micro Mill (Fritsch Corp., Kanagawa, Japan). The zirconia balls (diameter: 10 mm) were added to recrystallized CLZ containing sodium docusate and low-substituted MC and then crushed with the Pulverisette 7 for 24 h (400 rpm). The experiment was conducted at 18-21˚C (room temperature) (16).

Measurement of particle size, number and image in CLZ. The CLZ nanoparticle was evaluated using a nanoparticle size analyzer (SALD-7100; Shimadzu Co., Kyoto, Japan; refractive index 1.60-0.10i), a nanoparticle tracking size analyzer (Nanosight LM10; Malvern Instruments Ltd., Worcestershire, UK) and a scanning probe microscope (SPM-9700; Shimadzu Corp., Kyoto, Japan). In the SALD-7100, the total distribution in CLZ_{micro} and CLZ_{nano} was 48.3±0.312 mm, 0.064±0.047 mm, respectively (mean particle size ± SD) The particle size and number by the Nanosight was measured following: purification system of the water containing 100 μg CLZ_{nano} (500 μl) was injected into the sample chamber of the unit (Nanosight LM14; Malvern Instruments Ltd.) with a syringe. The suspension temperature in the sample chamber was 25˚C, the wavelength of the embedded laser was 405 nm (blue), the measurement time was 60 sec, and the viscosity of the suspension was 0.904-0.906 cP (water). The images of CLZ_{nano} were created by SPM-9700, and the particle size was measured from a cross section of the images of CLZ_{nano}.

Preparation of aqueous gel patches, gel and ointment containing CLZ_{nano}. The gel patches containing CLZ_{nano} (CLZ_{nano} gel patch) were prepared as described in Fig. 1A. The formulation of the CLZ_{nano} gel patches is described in Table I. In Fig. 1B, the completed aqueous gel patch containing CLZ_{nano} is shown. The CP gel and PEG ointment containing 0.5% CLZ_{micro} and 0.5% CLZ_{nano} were prepared by using Crbopol® 934 (1.5 w/w%) and polyethylene glycol (94.4 w/w%, PEG400: PEG 4,000=1:1), respectively.

In vitro skin penetration of CLZ gel patches. The *in vitro* skin penetration of CLZ from gel patches, CP gel, and PEG ointment experiment was evaluated by using the Franz diffusion cell (17). One day before the experiment, the hair on the abdominal area of 7-week-old Wistar rats was carefully shaved by using an electric clipper and razor. On the day of the experiment, sections of full-thickness abdominal skin (area: 3x3 cm^2) were extracted from the rats and the subcutaneous fat and other visceral debris were removed from the undersurface. The dermal side of the full-thickness skin was soaked in buffer (0.85% NaCl-10 mM phosphate buffer, pH 7.4) for 12 h at 4˚C to equilibrate the skin. Then, 0.3 g of 0.5% CLZ gel patches, CP gel, and PEG ointment was uniformly applied to the stratum corneum of the skin, which was then mounted on a Franz diffusion cell (reservoir volume, 12.2 ml; i.d. O-ring flange, 1.6 cm) and occluded with aluminum foil. The diffusion cells were maintained at a constant temperature of 37˚C for 48 h. The *in vitro* skin penetration experiment was performed as described above without a membrane filter. The amount of CLZ in the filtrates was determined by HPLC. Fifty microliters of the sample was added to 100 μl methanol containing 100 μg benzophenone (internal standard) and centrifuged at 15,000 rpm for 20 min. Ten μl of this solution was injected into an ODS column (3 μm, column size: 2.0x50 mm; Inertsil ODS-3; Shimadzu Co.) by using a Shimadzu LC-10AD system equipped with a CTO-6A column oven (Shimadzu Corp., Kyoto, Japan). The mobile phase consisted of a mixture of acetonitrile/methanol/water (35/15/50, v/v/v). The flow rate was 0.25 ml/min, the column temperature was 35˚C, and the wavelength used for detection was 254 nm. The obtained data were analyzed by using the following equations (equations 1 and 2):

$$J_c = \frac{Q}{A(t-\tau)} = \frac{D \cdot K_m \cdot C_c}{\delta} = K_p \cdot C_c$$

$$D = \frac{\delta^2}{6\tau}$$

where J_c, K_m, K_p, D, τ, d, C_c and A are the CLZ penetration rate, skin/preparation partition coefficient, penetration coefficient through the skin, diffusion constant within the skin, lag time, thickness of the skin (0.071 cm, mean of five independent

Table I. Formulations of the CLZ_{nano} gel patch.

Formulation	Content (w/w %)
Glycerin	15.00
Sodium polyacrylic acid	3.01
Aluminum hydroxide	0.98
Butylen glycol	0.61
Isostearic acid glyceres-25	0.31
Tartaric acid	0.24
Etylenediamintetraanmin acid-2Na	0.61
Methyl paraben	0.03
Propyl paraben	0.01
HPβCD	5.00
SM-4	0.50
Sodium docusate	0.20
CLZ_{nano} crystals	0.50

The CLZ_{nano} gel patch was obtained by adding these contents to purified water. CLZ_{nano}, cilostazol nanocrystals. HPβCD, 2-hydoxypropyl-β-cyclodextrin.

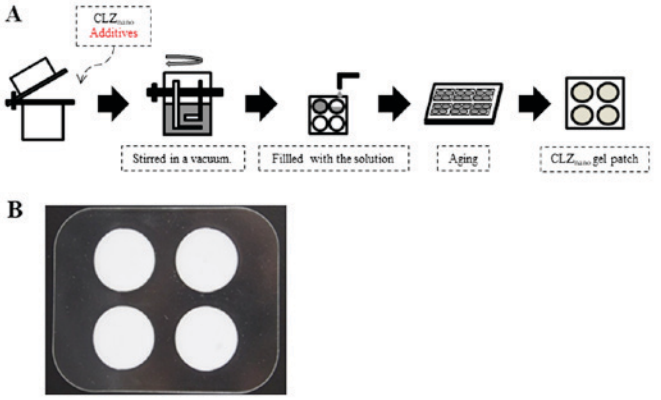

Figure 1. Preparation scheme of aqueous gel patches containing CLZ. (A) Preparation scheme of aqueous gel patches containing CLZ. (B) An image of aqueous gel patches containing CLZ_{nano}. CLZ, cilostazol; CLZ_{nano}, CLZ nanocrystals.

rats), amount of CLZ at time *t*, and the effective area of skin (2 cm^2). A nonlinear leastsquares computer program (MULTI) was used for the calculations.

In vitro skin penetration of CLZ_{nano} from gel patches. The *in vitro* skin penetration of CLZ_{nano} was analyzed Franz diffusion cell (17). In addition, a membrane filter (Durapore® Membrane Filter, pore size: 0.45 μm) was set under the skin to remove the debris from the skin. The number of CLZ_{nano} in the filtrates was determined as described above A calibration curve was generated from the relationship between the number of CLZ_{nano} and the amount of CLZ measured by HPLC method described above. The release of CLZ_{nano} was evaluated by the experimental method described above without the rat skin. The prepared analytical curve was used for the evaluation of the sample concentration from the ratio of the number of particles.

Analysis of pharmacokinetics of CLZ in rats. On the day prior to the experiment, the hair on the abdominal area of the 7-week-old Wistar rats was carefully shaved with an electric clipper and razor, and a cannula filled with 30 μg/ml heparin (silicone tubing; i.d., 0.5 mm, o.d., 1.0 mm) was inserted into the right jugular vein of the rats under pentobarbital anesthesia (40 mg/kg, intraperitoneally). A sheet of CLZ gel patches (0.3 g) and gel ointment was fixed on the shaved abdominal skin with an adhesive and immediately occluded with adhesive tape. Venous blood (100 μl) was collected from the jugular vein through the cannula between 0 and 48 h after the application of the CLZ gel patches and gel ointment (18). The blood was centrifuged at 15,000 rpm for 20 min at 4˚C to obtain, plasma, which was stored at -80˚C until analysis. The CLZ concentrations in the samples were determined by the HPLC method described above.

CLZ_{nano} gel patches, CLZ_{nano} CP gel, and CLZ_{nano} PEG ointment were applied to Wistar rats (n=3) at a dose of 0.15 g/sheet. The rats were allowed free access to water and food throughout the experiment. The blood samples (0.1 ml) were collected from the jugular vein at 0 (pre-dose), 2, 4, 6, 8, 24, 27, 30, 33, and 48 h after the administration. The serum samples were obtained by centrifugation at 15,000 rpm for 20 min and then stored at 4˚C until analysis. The CLZ concentration in the samples was determined by the HPLC method described above. The obtained data were analyzed by the using the following formula (equations 3 and 4):

$$C_{CLZ} = A\ e^{\alpha t} + B\ e^{\beta t}$$

$$C_{CLZ} = \frac{A\ k_a}{k_a\ \alpha} e^{\alpha t} + \frac{B\ k_a}{k_a\ \beta} e^{\beta t} - \left(\frac{A\ k_a}{k_a\ \alpha} + \frac{B\ k_a}{k_a\ \beta}\right) e^{k_a t}$$

where C_{CLZ} is the CLZ concentration of blood, *A* and *B* are the contribution rates, k_a is the rate content, and α and β are the elimination rate constants. The obtained data were analyzed by the simplex method and the damped Gauss-Newton method (18).

Statistical analysis. Unpaired Student's t-tests were used for statistical analysis and P-values less than 0.05 were considered significant. All data are expressed as the mean ± standard deviation (SD) or standard error of the mean (SE).

Results

Preparation of CLZ_{nano}. The particle size distribution of CLZ_{nano} is shown in Fig. 2A and B, and the particle size distribution of CLZ_{nano} is shown in Table II. The mean and mod particle sizes of CLZ_{nano} were 74.5±6.2 and 44.2±4.0 nm, respectively. The occupation percentage of nanocrystals with a diameter <200 nm diameter in CLZ_{nano} and CLZ_{micro} was 100 and 21%, respectively. Moreover, the percentage of nanocrystals with a diameter less than 100 nm CLZ_{nano} was 80±3.2%, (mean ± SE, n=5). The SPM images of the CLZ_{nano} dispersion are shown in Fig. 2C. The particle size of CLZ_{nano} was 66.45±5.35 nm (mean ± SE, n=5). Because ground CLZ_{nano} showed no aggregation, the similarity of the particle sizes between SPM and the nanoparticle tracking analyzer provided an indication of uniform quality of the nanocrystals in CLZ_{nano}.

Percutaneous penetration of CLZ released from CLZ_{micro} and CLZ_{nano} gel patches. The penetration profiles of CLZ

Table II. Ratio of nanoparticles (<1 μm) in CLZ_{nano} and CLZ_{micro}.

Distribution	CLZ_{nano} (nm)	CLZ_{micro} (nm)
Mean	74.5±6.2	236.6±35.4
Mode	44.2±4.0	144.5±26.7
SD	47.1±5.0	131.9±12.7
D10	40.0±4.1	93.4±30.3
D50	48.4±4.6	215.0±36.7
D90	144.8±10.6	447.4±44.4
Occupation % of nanoparticles number (<200 nm)	100	21

The occupation and distribution nanoparticles (<1 μm) was measured using Nanosight. The data are presented as the mean ± standard error (n=5). CLZ, cilostazol; CLZ_{nano}, CLZ nanocrystals; CLZ_{micro}, CLZ powder; SD, standard deviation.

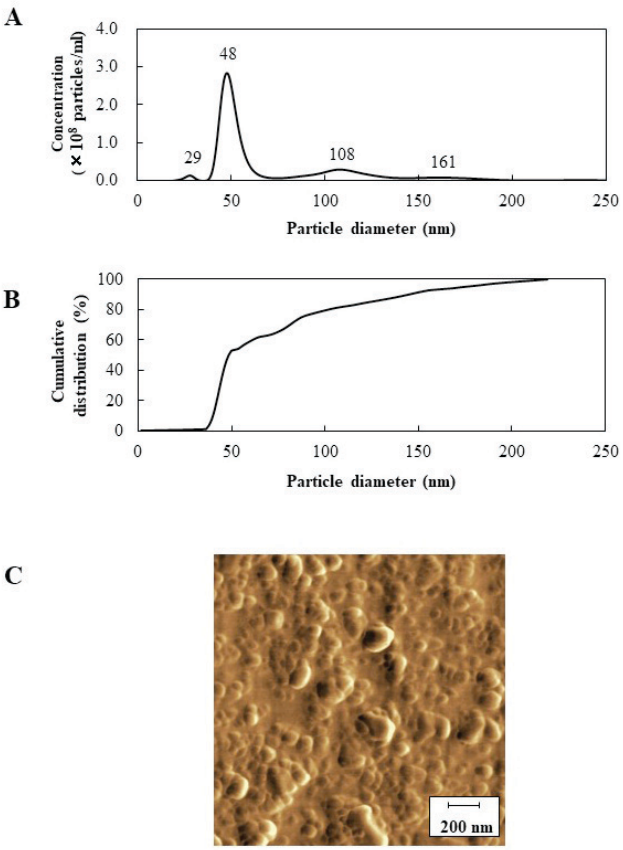

Figure 2. Frequency size distribution, cumulative size distribution and images of CLZ_{nano}. CLZ_{nano} were suspended using purified water. (A) Frequency size distribution of CLZ_{nano}. The numbers show the indicated peak size (29, 48, 108 and 161 nm, respectively). (B) Cumulative size distribution of CLZ_{nano}. (C) Image of CLZ_{nano} (scale bar=200 nm). The mean particle size of CLZ_{nano} was 66.45±5.35 nm (mean ± standard divation; n=5). CLZ, cilostazol; CLZ_{nano}, CLZ nanocrystals.

through rat skin after the application of CLZ_{micro} and CLZ_{nano} gel patches and ointments are shown in Fig. 3, and the pharmacokinetic parameters calculated from the *in vitro* skin penetration data are summarized in Table III. Regarding particle size, a significant difference was found in the CLZ gel patches and ointment between the CLZ_{nano} and CLZ_{micro} groups; with respect to gel properties, a significant difference was found in the pharmacokinetic parameters. The amount of penetrated CLZ increased linearly after the application of either CLZ gel patches or ointment into the donor chambers, and the penetration rate (J_c) of CLZ_{nano} gel patch was 1.4-fold higher than that of the CLZ_{micro} gel patch. The penetration coefficient through the skin (K_p) and the skin/preparation partition coefficient (K_m) values of the CLZ_{nano} gel patches and ointment were significantly higher than those of the CLZ_{micro} gel patches and ointment. The lag times (τ) for the CLZ_{micro} and CLZ_{nano} gel patches and ointments were different. In contrast, the pharmacokinetic parameters of CLZ in the gel patches were markedly increased compared with those of the CLZ CP gel and PEG ointment.

The calibration curve between the number of CLZ_{nano} with an average particle diameter of 200 nm and the concentration of CLZ is shown in Fig. 4. The calibration curve was shown as a straight line with the slope of 4.68×10^{-8} mg/particle number and correlation coefficient (r)=0.972. In Fig. 5, the profiles of the penetrated CLZ_{nano} in the *in vitro* skin penetration experiment are shown. The nanocrystals with an average particle diameter <200 nm were detected in a reservoir chamber, and the number of nanocrystals increased with the incubation time. As shown in Fig. 5, the penetration rate (J_c) of the CLZ_{nano} gel patch and the CLZ_{micro} gel patch was 769.9 and 367.6 ng/cm^2/h, respectively. Therefore, 98% of penetrated CLZ after the application of CLZ_{nano} gel patch to rat skin was observed in the nanocrystal form; for the CLZ_{micro} gel patch, the value was 96%.

The absorption profiles of CLZ through rat skin *in vivo* after the application of CLZ_{nano} gel patches and ointments are shown in Fig. 6; Table IV summarizes the pharmacokinetic parameters calculated from the *in vivo* percutaneous absorption data. The plasma concentration of CLZ increased after the application of the CLZ_{nano} gel patches, and the apparent absorption rate constant (k_a) and $AUC_{0\text{-}48\ h}$ values in the skin of rats administered the CLZ_{nano} gel patches were significantly higher than those of rats administered the CLZ_{nano} gel and ointment, but the lag time was decreased.

Discussion

Sparingly water-soluble medicaments have poor oral absorption. We have previously designed drug nanocrystals by a combination of recrystallization and the breakdown method using a ball mill (16) and shown that CLZ_{nano} enhanced drug bioavailability in the small intestine of rats (16).

In this study, we confirmed the diameter of CLZ_{nano} by using a nanoparticle tracking size analyzer and a scanning probe microscope. Moreover, we designed new transdermal drug delivery formulations containing CLZ_{nano} using hydrophilic polymeric gelling agents, and investigated the penetration of CLZ through rat skin.

First, we attempted to measure the diameter of the CLZ_{nano}. Recently, nanocrystals have been thoroughly evaluated for their potential as a tool to carry drug payloads, image contrast agents, or gene therapeutics for disease diagnosis and treatment, with the primary focus on cancer (19-27). It is known

Table III. Pharmacokinetic parameters for *in vitro* percutaneous penetration of CLZ from CLZ_{nano} gel patch and carbopol gel and polyethylene glycol ointments.

A, Patch

Preparation	τ (h)	D (x10^{-4} cm^2/h)	J_c (ng/cm^2/h)	K_p (x10^{-4} cm/h)	K_m
CLZ_{nano} gel	1.75±0.46[a]	4.81±1.83[a]	686±51.90[a,b]	1.37±0.10[a,b]	2.03±0.66[a,b]
CLZ_{micro} gel	1.82±0.46	4.61±1.83	474±112.7	0.95±0.23	1.46±0.36

B, Ointment

Preparation	τ (h)	D (x10^{-4} cm^2/h)	J_c (ng/cm^2/h)	K_p (x10^{-4} cm/h)	K_m
CLZ_{nano} CP gel	3.75±1.78	3.04±2.33	306±67.40	0.88±0.19	0.03±0.01
CLZ_{micro} CP gel	5.52±1.95	1.83±1.10	104±29.20	0.30±0.08	0.01±0.01
CLZ_{nano} PEG	6.75±0.64	1.47±0.16	160±11.80	0.46±0.03	0.02±0.01
CLZ_{micro} PEG	N.D.	N.D.	N.D.	N.D.	N.D.

Parameters were calculated according to equations 1 and 2. The compositions of the CLZ gel patch are shown in Table I. The data are presented as means ± standard errpr of 3 independent rats. [a]P<0.05 vs. other preparation without CLZ_{micro} gel patch; [b]P<0.05 vs. CLZ_{micro} gel patch. CLZ, cilostazol; CLZ_{nano}, CLZ nanocrystals; CLZ_{micro}, CLZ powder; CP, carbopol; PEG, polyethylene glycol; J_c CLZ penetration rate; K_p, penetration coefficient through the skin; K_m, skin/preparation partition coefficient; τ, lag time; D, diffusion constant within the skin; N.D., not detectable.

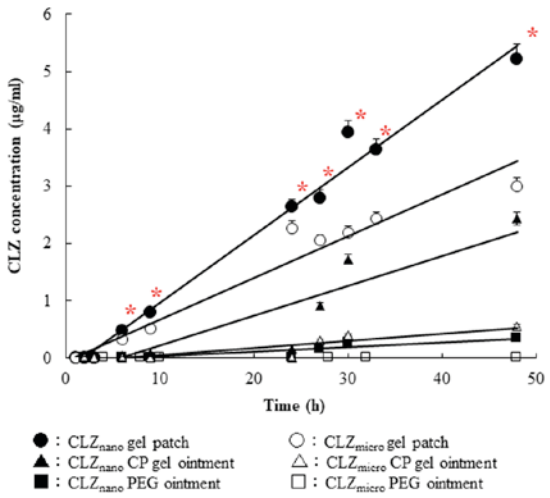

Figure 3. Changes in CLZ concentration following the application of CLZ aqueous gel patch, gel and ointment. CLZ_{micro} gel patch (open circles), CLZ_{micro} gel patch-applied rat skin; CLZ_{nano} gel patch (closed circles), CLZ_{nano} gel patch-applied rat skin; CLZ_{micro} CP gel (open triangles), CLZ_{micro} CP gel-applied rat skin; CLZ_{nano} CP gel (closed triangles), CLZ_{nano} CP gel-applied rat skin; CLZ_{micro} PEG ointment (open squares), CLZ_{micro} PEG ointment-applied rat skin; CLZ_{nano} PEG ointment (closed squares), CLZ_{nano} PEG ointment-applied rat skin. Data are presented as the mean ± standard error (n=3-5). *P<0.05 vs. the CLZ_{micro} gel patch groups within each category. CLZ, cilostazol; CLZ_{nano}, CLZ nanocrystals; CLZ_{micro}, CLZ powder; PEG, polyethylene glycol; CP, carbopol.

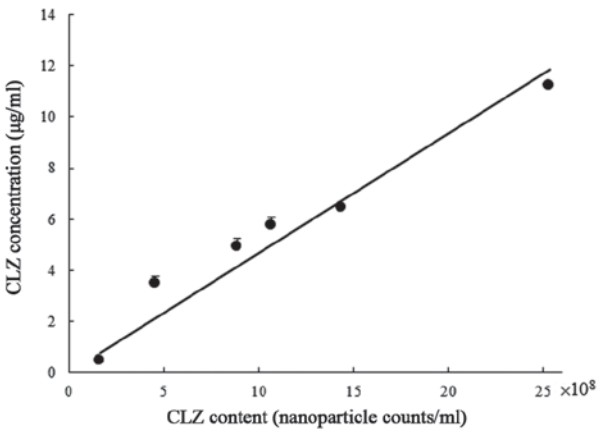

Figure 4. Correlation curve between the number of CLZ nanocrystals and the concentration of CLZ. Data are presented as the mean ± standard error (n=3-5). CLZ, cilostazol.

that the behavior of nanoparticles <100 nm is unique (19). Nanocrystals possess different physical and chemical properties as well as optical and electromagnetic characteristics (19). The diameter of CLZ_{nano} was measured by using a nanoparticle tracking size analyzer and a scanning probe microscope. In this study, the mean diameter of CLZ_{nano} measured by using a tracking size analyzer was <100 nm, but the cumulative distribution indicated that approximately 20% of the CLZ_{nano} were >100 nm (Fig. 2A and B). Therefore, we visually evaluated the images of the CLZ_{nano} captured by using a scanning probe microscope to confirm the size of the nanocrystals visually. In these images, nanocrystals with a primary particle size of 30-80 nm were clearly visible and comprised a majority of the primary particles and a few secondary particles comprising agglomerated or flocculated primary particles (Fig. 2C). However, the secondary particles are moved and crushed by the extremely small power of the probe cantilever of the SPM. This suggests that the secondary particles are transient and crushed to the primary particles, and that the number of secondary particles that are >100 nm is almost negligible.

In this study, we prepared an aqueous gel patch containing CLZ_{nano}, with excellent drug release properties, skin

Table IV. Pharmacokinetic parameters for *in vivo* percutaneous absorption of CLZ following the application of CLZ_{nano} gel patch and ointments.

Preparation	τ (h)	k_a (/h)	A (μg/ml)	B (μg/ml)	AUC (μg/ml)	MRT (h)	BA (%)
CLZ_{nano} gel patch	0.71±0.03[a]	19.03±2.08[a,b]	0.15±0.16	99.08±22.10[a,b]	7.51±0.48[a,b]	34.36±3.09[a,b]	63.3±0.6[a,b]
CLZ_{nano} CP gel ointment	2.66±1.09	11.70±4.08	8.06±1.14	4.99±1.3	2.92±0.94[b]	25.05±0.60	24.5±1.3[b]
CLZ_{nano} PEG ointment	5.75±0.55	7.06±0.15	4.58±0.28	3.81±0.47	1.53±0.35	29.86±2.05	12.9±0.2

Parameters were calculated according to equations 3 and 4. The compositions of the CLZ_{nano} gel patch are shown in Table I. The data are presented as the mean ± standard error of 3 independent rats. [a]P<0.05 vs. CLZ_{nano} CP gel for each category; [b]P<0.05 vs. CLZ_{nano} PEG ointment for each category. CLZ, cilostazol; CLZ_{nano}, CLZ nanocrystals; CLZ_{micro}, CLZ powder; CP, carbopol; PEG, polyethylene glycol; τ, lag time; k_a, absorption rate constant; A, contribution rates in the α-phase; B, contribution rates in the β-phase; BA, bioavailability; AUC, area under the curve; MRT, mean residence time.

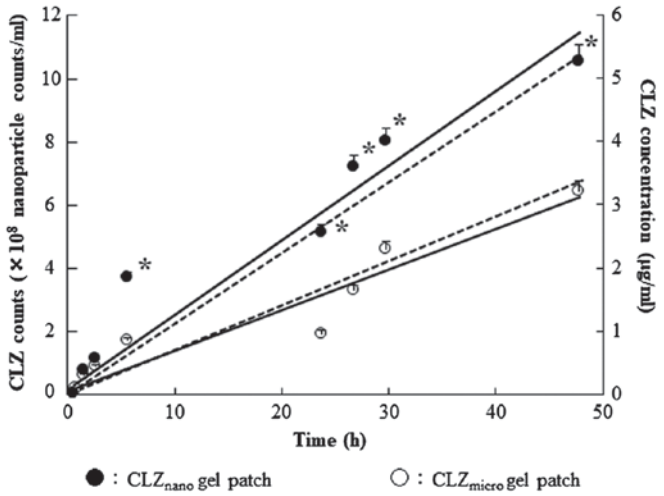

Figure 5. Changes in solution CLZ nanocrystals counts following application of CLZ aqueous gel patch. CLZ_{micro} gel patch, CLZ_{micro} gel patch-applied rat skin; CLZ_{nano} gel patch, CLZ_{nano} gel patch-applied rat skin. Solid lines are shown as fitting curves using equation 1 and the penetrated content profiles of CLZ nanocrystal particles. The dotted lines are shown as fitting curves using Equation 1 and penetrated CLZ concentration calculated by the conversion factor. The particle size of CLZ_{nano} following percutaneous penetration remain nano order (216.1±10.7 nm). Dotted lines are the actual value of CLZ from *in vitro* skin penetration experiments. Data are presented as the mean ± standard error (n=3-5). *P<0.05 vs. CLZ_{micro} gel patch group. CLZ, cilostazol; CLZ_{nano}, CLZ nanocrystals; CLZ_{micro}, CLZ powder.

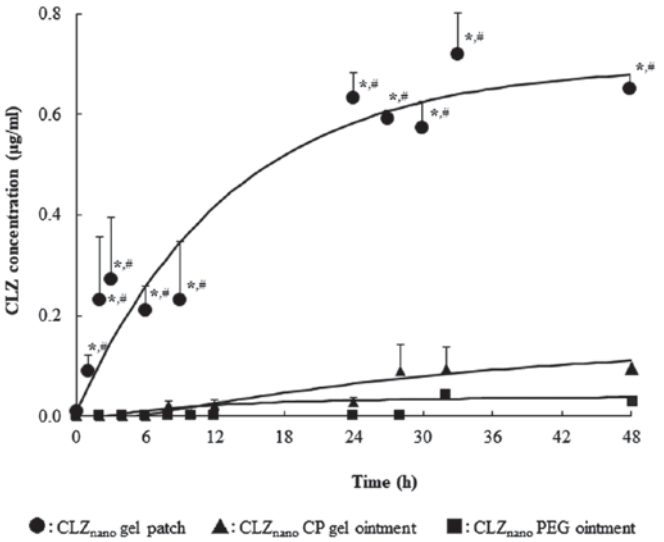

Figure 6. Plasma CLZ concentrations following the application of CLZ_{nano} aqueous gel patches and gel ointments. The rats were fasted for 18 h prior to the experiments; however they were given free access to water. CLZ_{nano} aqueous gel patch or gel ointment (3 mg/kg) were applied to the rats. Solid lines represent the fitting curves calculated from equations 3 and 4. CLZ_{nano} gel patch, CLZ_{nano} gel patch-applied rat skin; CLZ_{nano} CP gel ointment, CLZ_{nano} CP gel ointment-applied rat skin; CLZ_{nano} PEG gel ointment, CLZ_{nano} PEG gel ointment-applied rat skin. Data are presented as the mean ± standard error (n=3). *P<0.05 vs. CLZ_{nano} CP gel ointment groups; #P<0.05 vs. CLZ_{nano} PEG ointment groups. CLZ, cilostazol; CLZ_{nano}, CLZ nanocrystals; CLZ_{micro}, CLZ powder; PEG, polyethylene glycol; CP, carbopol.

permeability and skin permeation rate, quantitative drug release even in long term application and showed excellent retention. The data indicated that the milled CLZ_{nano} were homogeneous with a narrow particle size distribution. It is reported that nanoparticles from organic compounds are able to move through the spaces between the cells (28). In a previous study, we reported that recrystallization was suitable for the preparation of nanocrystals by using mill methods (16). These results suggested that the CLZ released from the CLZ_{nano} gel patches was in a nanocrystal state.

The successful delivery of a drug across the skin requires a high-performance drug delivery device (29). Clinically, the most common bases for transdermal therapeutic systems are CP gel and PEG ointment, which are used pharmaceutically as lubricants and also as carriers for many drugs (30,31). Aqueous gel patches using high molecular weight polymer have attracted attention as a new base in the cosmetics industry (32). Therefore, we prepared an aqueous gel patch containing CLZ_{nano} by using high molecular weight polymer absorbent, which has excellent drug release and skin permeation properties, skin permeation rate, quantitative release of a drug, even in long term application and with excellent retention, which allowed the uniform incorporation of the CLZ_{nano}. As shown by the above results, the gel patch using aqueous high molecular weight polymer absorbents shows excellent release properties and sustainability against rat skin and are subsequently extremely useful as a transdermal absorption base.

These results show that the formula developed in this study was suitable for the preparation of aqueous gel patches

containing CLZ_{nano}. The diffusion constant within the penetration rate (J_c), the penetration coefficient through the skin (K_p), and the skin/preparation partition coefficient (K_m) for the CLZ_{nano} gel patch were all significantly higher than those of the CLZ_{micro} gel patch, CLZ_{nano} and CLZ_{micro} gel ointment. Only lag time of CLZ_{nano} gel patch is shorter than others (Fig. 3, Table III). These results suggested that the CLZ_{nano} gel patches were exceptionally well suited for the base of percutaneous absorption type formulation.

In addition to this, we attempted to clarify the absorption mechanism by counting the number of CLZ_{nano} that permeated the rat skin from the CLZ gel patches. According to the calibration straight line and the penetration profiles of CLZ_{nano}, a positive correlation was found between the number of CLZ_{nano} and the penetration of CLZ. Moreover, the predicted values that were calculated from the number of CLZ_{nano} and actual measurements were almost the same quantities (Figs. 4 and 5). These results suggested that the CLZ_{nano} smaller than 100 nm were transferred through the spaces in rat skin and into peripheral blood vessels. To the best of our knowledge, this is the first report to elucidate the permeation mechanism of nanoparticles in the percutaneous absorption experiment. Thus, we are now conducting a more detailed investigation of some details about the absorption mechanism of CLZ_{nano}.

In the *in vivo* study, the CLZ concentrations in the plasma of rats administered the CLZ_{nano} gel patches were also significantly higher than those of rats administered the CLZ_{nano} CP gel and PEG ointment (Table IV, Fig. 6). In this study, we have shown that the supply of CLZ from the CLZ_{nano} gel patches was higher than that from the CLZ_{nano} CP and PEG gel ointment. Therefore, the abundant supply of CLZ from the CLZ_{nano} gel patches may be related to the CLZ concentrations in the plasma. These results showed that the characteristics of the CLZ_{nano} gel patches in skin differ and suggested that the effects of local and systemic therapy were greater after the application of the CLZ_{nano} gel patches than the CLZ_{nano} CP and PEG gel ointment. In addition, it is important to clarify a suitable formulation for the transdermal therapeutic system for ischemic stroke symptoms using CLZ_{nano}. Therefore, we are now investigating the therapeutic effects of transdermal systems by using CLZ_{nano} and various additives on ischemic stroke symptoms.

In conclusion, we have developed a new aqueous gel patch system that includes CLZ_{nano} by using recrystallization and a planetary micro mill. The penetration of CLZ is attributed to the nanoscale crystals. The percutaneous penetration of CLZ from the CLZ_{nano} gel patches through the rat skin was significantly better than that from the CLZ_{nano} CP gel and PEG ointment. Moreover, we have clarified the mechanism of the transparency system of CLZ_{nano} through the rat skin. Thus, our findings suggest that a transdermal therapeutic system using nanocrystals may enable the application of medications without high systemic levels to provide an efficient and effective therapy and to spare patients from unwanted side effects. A transdermal formulation using CLZ_{nano} may provide a delivery option for clinical treatment of ischemic stroke symptoms.

References

1. Kimura Y, Tani T, Kanbe T and Watanabe K: Effect of cilostazol on platelet aggregation and experimental thrombosis. Arzneimittelforschung 35: 1144-1149, 1985.
2. Kanbayashi J, Liu Y, Sun B, Shakur Y, Yoshitake M and Czerwiec F: Cilostazol as a unique antithrombotic agent. Curr Pharm Des 9: 2289-2302, 2003.
3. Bramer SL and Forbes WP: Relative bioavailability and effects of a high fat meal on single dose cilostazol pharmacokinetics. Clin Pharmacokinet 2 (37 Suppl): S13-S23, 1999.
4. Jinno J, Kamada N, Miyake M, Yamada K, Mukai T, Odomi M, Toguchi H, Liversidge GG, Higaki K and Kimura T: Effect of particle size reduction on dissolution and oral absorption of a poorly water-soluble drug, cilostazol, in beagle dogs. J Control Release 111: 56-64, 2006.
5. Jinno J, Kamada N, Miyake M, Yamada K, Mukai T, Odomi M, Toguchi H, Liversidge GG, Higaki K and Kimura T: In vitro-in vivo correlation for wet-milled tablet of poorly water-soluble cilostazol. J Control Release 130: 29-37, 2008.
6. Rasenack N and Müller BW: Micron-size drug particles: Common and novel micronization techniques. Pharm Dev Technol 9: 1-13, 2004.
7. Gotoh F, Tohgi H, Hirai S, Terashi A, Fukuuchi Y, Otomo E, Shinohara Y, Itoh E, Matsuda T, Sawada T, *et al*: Cilostazol stroke prevention study: A placebo-controlled double-blind trial for secondary prevention of cerebral infarction. J Stroke Cerebrovasc Dis 9: 147-157, 2000.
8. Sugibayashi K: Development & Applications of Transdermal Drug Delivery Systems. CMC publishing Company, Tokyo, pp167-176, 2011.
9. Honeywell-Nguyen PL and Bouwstra JA: Vesicles as a tool for transdermal and dermal delivery. Drug Discov Today Technol 2: 67-74, 2005.
10. Walters KA and Roberts MS: The structure and function of the skin. Marcel Dekker, New York, NY, pp1-40, 2002.
11. Cevc G and Vierl U: Nanotechnology and the transdermal route: A state of the art review and critical appraisal. J Control Release 141: 277-299, 2010.
12. Scheuplein RJ: Mechanism of percutaneous absorption. I. Routes of penetration and influence of solubility. J Invest Dermatol 45: 334-346, 1965.
13. Watanabe T: The present conditions and the prospects of a skin applications drug. Drug Delivery System 22: 450-457, 2007.
14. Tsujimoto H, Hara K, Yokoyama T, Yamamoto H, Takeuchi H, Kawashima Y, Akagi K, Miwa N and Haung CC: Percutaneous absorption study of biodegradable PLGA nano-spheres via human skin biopsies. J Soc Powder Technol 41: 867-875, 2004.
15. Bal SM, Ding Z, van Riet E, Jiskoot W and Bouwstra JA: Advances in transcutaneous vaccine delivery: Do all ways lead to Rome? J Control Release 148: 266-282, 2010.
16. Yoshioka C, Ito Y and Nagai N: An oral formulation of cilostazol nanoparticles enhances intestinal drug absorption in rats. Exp Ther Med 15: 454-460, 2017.
17. Franz TJ: Percutaneous absorption on the relevance of in vitro data. J Invest Dermatol 64: 190-195, 1975.
18. Nagai N, Iwamae A, Tanimoto S, Yoshioka C and Ito Y: Pharmacokinetics and antiinflammatory effect of a novel gel system containing ketoprofen solid nanoparticles. Biol Pharm Bull 38: 1918-1924, 2015.
19. DeLouise LA: Applications of nanotechnology in dermatology. J Invest Dermatol 132: 964-975, 2012.
20. Gao X, Cui Y, Levenson RM, Chung LW and Nie S: In vivo cancer targeting and imaging with semiconductor quantum dots. Nat Biotechnol 22: 969-976, 2004.
21. Moghimi SM, Hunter AC and Murray JC: Nanomedicine: Current status and future prospects. FASEB J 19: 311-330, 2005.
22. Al-Jamal WT, Al-Jamal KT, Tian B, Cakebread A, Halket JM and Kostarelos K: Tumor targeting of functionalized quantum dot-liposome hybrids by intravenous administration. Mol Pharm 6: 520-530, 2009.
23. Boisselier E and Astruc D: Gold nanoparticles in nanomedicine: Preparations, imaging, diagnostics, therapies and toxicity. Chem Soc Rev 38: 1759-1782, 2009.
24. Debbage P: Targeted drugs and nanomedicine: Present and future. Curr Pharm Des 15: 153-172, 2009.
25. Huang HC, Barua S, Sharma G, Dey SK and Rege K: Inorganic nanoparticles for cancer imaging and therapy. J Control Release 155: 344-357, 2011.
26. Huang X, Peng X, Wang Y, Wang Y, Shin DM, El-Sayed MA and Nie S: A reexamination of active and passive tumor targeting by using rod-shaped gold nanocrystals and covalently conjugated peptide ligands. ACS Nano 4: 5887-5896, 2010.

27. Ilbasmiş-Tamer S, Yilmaz S, Banoğlu E and Değim IT: Carbon nanotubes to deliver drug molecules. J Biomed Nanotechnol 6: 20-27, 2010.
28. Zhang LW, Yu WW, Colvin VL and Monteiro-Riviere NA: Biological interactions of quantum dot nanoparticles in skin and in human epidermal keratinocytes. Toxicol Appl Pharmacol 228: 200-211, 2008.
29. Garala K, Faldu N, Basu B, Bhalodia R, Mehta K and Joshi B: Chemical penetration enhancement. J Pharm Res 2: 1804-1808, 2009.
30. Nishihata T, Kamada A, Sakai K, Takahashi K, Matsumoto K, Shinozaki K, Tabata Y, Keigami M, Miyagi T and Tatsumi N: Percutaneous absorption of diclofenac in rats and humans: Aqueous gel formulation. Int J Pharm 46: 1-7, 1988.
31. Ahmed TA, Ibrahim HM, Ibrahim F, Samy AM, Fetoh E and Nutan MT: In vitro release, rheological, and stability studies of mefenamic acid coprecipitates in topical formulations. Pharm Dev Technol 16: 497-510, 2011.
32. Goddard ED and Gruber JV (eds): Principles of polymer science and technology in cosmetics and personal care. Marcel Dekker, Inc., New York-Basel, 1999.